IDEA PROJECT FINAL REPORT
Contract ITS-8

IDEA Program
Transportation Research Board
National Research Council

February 8,1995

INTELLIGENT TRANSPORTATION APPLICATIONS OF LASER OPTICS OPEN AIR COMMUNICATION SYSTEM

Sheldon Chang
State University of New York
Stony Brook

The ITS-IDEA program is jointly funded by the U.S. Department of Transportation's Federal Highway Administration, National Highway TrafEc Safety Administration, and Federal Railroad Administration. For information on the IDEA Program contact Dr. K. Thirumalai, IDEA Program Manager, Transportation Research Board, 2101 Constitution Avenue N.W., Washington, DC 20418 (phone 202-334-3568, fax 202-334-3471).

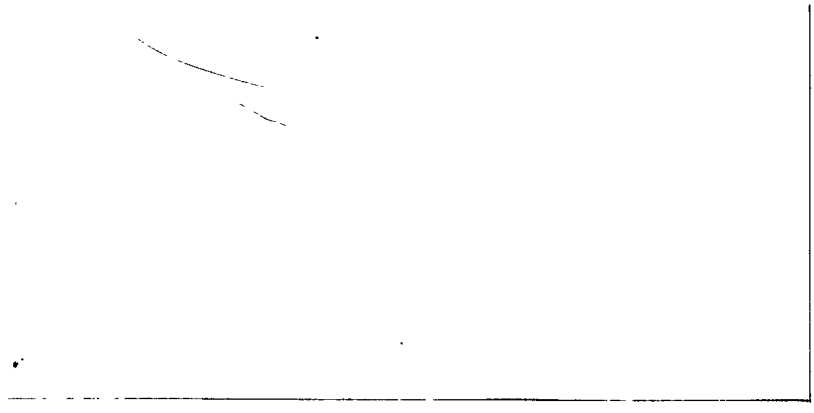

INNOVATIONS DESERVING EXPLORATORY ANALYSIS (IDEA) PROGRAMS MANAGED BY THE TRANSPORTATION RESEARCH BOARD (TRB)

This investigation was completed as part of the ITS-IDEA Program which is one of three IDEA programs managed by the Transportation Research Board (TRB) to foster innovations in surface transportation. It focuses on products and result for the development and deployment of intelligent transportation systems (ITS), in support of the U.S. Department of Transportation's national ITS program plan. The other two IDEA programs areas are Transit-IDEA, which focuses on products and results for transit practice in support of the Transit Cooperative Research Program (TCRP), and NCHRP-IDEA, which focuses on products and results for highway construction, operation, and maintenance in support of the National Cooperative Highway Research Program (NCHRP). The three IDEA program areas are integrated to achieve the development and testing of nontraditional and innovative concepts, methods and technologies, including conversion technologies from the defense, aerospace, computer, and communication sectors that are new to highway, transit, intelligent, and intermodal surface transportation systems.

ACKNOWLEDGEMENTS

This work could not have been carried out without ITS-IDEA support. The writer is most grateful to members of the ITS-IDEA advisory committee and especially to Dr.'s K. Thirumalai and William Agnew, and to Mr. Keith Gates for their many very helpful suggestions.

TABLE OF CONTENTS

1. EXECUTIVE SUMMARY

This IDEA project explores the applications of infra-red lightwaves in ITS communication and automated vehicle control. Two IDEA products emerge from this work: a communication system between the highway system and the vehicles, and an automated highway system (AI-IS) in which the vehicle operates by itself without the need of an operator or driver.

The devices required in the vehicle for the above two applications can be combined into one vehicle terminal (VT) which would significantly increase the IDEA product's utility to cost ratio. With millions of equipped vehicles on the highway, the total cost of the proposed system's infrastructure on the highway side will be no more than a few percent of the total cost of these vehicle terminals. The proposed system thus furthers the ISTEA goal that ITS implementation should be largely paid for by private investment.

Inexpensive semiconductor lasers of the GaAs family with a wavelength between 0.65 to 2 micrometers are used in cost-conscious commercial applications, such as bar-code scanners. Because lightwaves in the visible wavelength range are both disturbing and harmful to the human eye, our research is concentrated in the infra-red wavelength range (IR) of 1 to 2 micrometers.

The currently predominant research and development efforts for ITS signaling and sensing applications are in the millimeter wavelength range (MMW), at the high end of what is generally considered to be "radio frequency" (RF). These RF wavelengths are thousands of times longer than the operating wavelengths of inexpensive IR semiconductor lasers. The shorter IR wavelength means a proportionally higher resolution in both space and time than would be possible with RF devices. For AHS, higher resolution means a faster and more accurate determination of the vehicle' s position and direction of travel relative to the lane center as well as the relative distance and speed of any obstacle in the vehicle's path. For communication, a higher time resolution means proportionally higher information exchange rate. A higher resolution in transmitting and receiving beam directions means less required signal power and a higher signal to noise ratio as well as elimination of interference.

The above discussion does not imply that a millimeter wave (MMW) device is necessarily, thousands of times lower in its resolution than an IR device. In an actual design, the resolution of a MMW device must be stretched almost to its theoretical limit to meet ITS requirements. In contrast, since ITS requirements are well within lR's resolution range, design emphasis can be placed on other factors such as size, cost, and reliability.

A recent development is the possibility of a directed and focusing laser (DAFL) [l]. It is well known that the direction of an RF beam, either transmitting or receiving, can be controlled by changing the relative phase of an array of antenna elements (a "phased array"). The directed and focusing laser (DAFL) can be described as an electronically controlled phased array antenna for lightwaves. Because of the short wave length of light a DAFL can be realized as an array of phase-controlled optical paths on a single semiconductor chip. This technology can be used to very substantially reduce the size, manufacturing cost, and reliability of the proposed VTs (just as the integration of computer components onto semiconductor chips has had this effect on computers).

Figure 1 illustrates a system for communication between a highway and its vehicles. On the highway side is a system of infra-red lightwave transmitting-receiving terminals (HWT) which are linked via commercial telephone lines, and/or computer communication networks to a traffic operations center (TOC). Each terminal has a built-in two-way signal storage and forward device which could be implemented in a specially programmed microprocessor. The highway terminal is mounted on an overhead structure (e.g. an overhead bridge) and a similar terminal device (VT) is installed on each vehicle. The terminals can communicate with each other as the vehicle passes under the overhead structure without stopping or slowing down, as shown in Figure 1.

Figure 2 illustrates an automated highway system (AHS) which takes control of the driving while allowing the driver to work or rest. It is a common practice to implant small bumps on highway lane dividing lines to wake up a dozing driver; our proposed system is to implant semi-spherical infrared reflecting objects instead. DAFLs on the vehicle automatically beam at the reflecting objects, as shown in Figure 2. Thus it is possible to generate four steering signals in the system: the angles and distances to the reflecting objects on the left and right lane dividers. A frontal laser signal could also be designed to track the position of the vehicle ahead for longitudinal collision avoidance. These five signals are sufficient for guiding a car in an automated system.

Our investigation shows that:

- No less then one Megabyte of data can be exchanged safely and reliably each time a HWT is passed under all weather and traffic conditions. This is approximately the information content of the Holy Bible.

- With the five guiding signals described above the vehicle can be controlled to cruise smoothly near the center of the lane, even while the road twists and turns.

The consumer's propensity to purchase the VT required for this system is enhanced by the ability of this equipment *to* facilitate delivery of several ITS user services, several of which are listed below. Because of the system's huge information transfer capability the first four services below can be combined in one exchange package between the VT and the HWT. Returned information can then be displayed on an inexpensive Liquid Crystal Diode (LCD) display as desired by the vehicle's operator. We propose that this IDEA concept be developed to complement other ITS technologies (e.g. GPS, microwave, etc.).

Automatic toll collection

At toll collection stations, a vehicle containing a VT can pass directly through gates equipped with HWT without slowing or stopping. The vehicle's identity, time, and toll charge are automatically recorded in the HWT's disk memory and billed periodically to the vehicle's owner.

Car-pool and minibus information

Terminals are provided at road-side car-pool lots. A potential share rider inserts his personal identification card and enters his/her destination into a terminal which communicates with a nearby HWT. A vehicle or minibus looking for a passenger picks up the list of potential passengers and their destinations by pushing a button shortly before encountering the HWT. The list of potential passengers is then quickly displayed on his (or her) monitor. If a successful pickup is made, the vehicle and new passengers insert their cards into the car pool terminal to notify the highway system. The system is not only a convenience, but it also helps to reduce foul-play by letting both parties know that the identities, time, and place of the share-ride event are on official record.

Road condition, motel, restaurant, fuel, "best route" and other needed information

Information requested from a VT can be displayed on a monitor after one encounter with an HWT.

Commercial Vehicle Operations

For vehicles belonging to a commercial fleet, the vehicle's identity and time of its passing through a HWT gate along with directives or instructions from Fleet Control to the vehicle can be exchanged during each passing.

Automated driving

Automated lane-keeping and headway maintenance allows the driver to rest, relax, or perform his or her work en-route, under all driving conditions including congested traffic, e.g. commuting near large cities.

2. PROBLEM STATEMENT

This IDEA project explores the applications of infrared lightwaves in ITS communication and automated vehicle control. Two IDEA products emerge from this work: a communication system between the traffic operations center (TOC) and vehicles on its highways, and an automated highway system (AHS) in which a vehicle can control its position within a lane and relative to other vehicles without driver assistance.

There are two objectives of our IDEA project: to explore the design of economically feasible IDEA products and to prove the technical feasibilities of these products for their intended applications.

2.1 TECHNICAL FEASIBILITIES

2.1.1 Feasibility of the Communication System

The feasibility conditions are the following:

- sufficiently strong laser signal to assure satisfactory communication under all weather conditions;
- sufficiently weak laser signal to assure a margin of safety to the eye at all times; and
- system operability under all traffic and weather conditions.

This last condition implies that the system's operation will not impede traffic flow in any way and that, even in a traffic jam, there will be no cross-talk or interference between communication links.

2.1.2 Feasibility of the Automated Highway System

The AHS feasibility conditions are the following:

- sufficiently simple and rugged steering algorithms for reliable operation;
- high dynamic stability so that any initial deviation from the guided path would decrease with time; and
- sufficient accuracy in steering signals so that the vehicle would stay close to the center of the lane.

2.1.3 Scientific and Technological Feasibility of the DAFL Device

The DAFL device feasibility conditions are:

- material feasibility (selection of semiconductor materials which have the desired dependence of phase-shift on carrier density), and
- design feasibility (a DAF'L can be designed and mass-produced to meet the system requirements).

2.2 ECONOMIC FEASIBILITIES

There are two economic feasibility conditions:

- the vehicle terminal devices for communication and AHS are to be mass-produced at a price not much above an expensive accessory, e.g. a personal computer or a musical system; and
- the total cost on the highway system, which include installation and maintenance, should be low compared to the total cost of the terminal equipment on all vehicles using them.

The first condition is important to the wide-spread use of our LOOC product. The second condition is important for its nation-wide and world-wide adoption. Most economists agree that public or government spending is a drain on the economy because the money has to come from taxation while private spending on a new and useful product is a boost to the economy.

3. RESEARCH APPROACH

This section summarizes calculations which investigate the feasibility of communication, automated vehicle control, and the associated enabling devices (VT and HWT terminals). The feasibility conditions listed in section 2 are evaluated and system design limitations are explored for both communication system and AI-IS functional requirements. There is also a discussion of issues involved in the design and manufacture of the hardware needed for system implementation.

An extensive appendix covering design and fabrication of the DAFL device is available as a supplement to this paper to further support the analysis in this section.

3.1 BASIC CONDITIONS FOR COMMUNICATION

The design limitations to be established here relate to:

- sufficiently strong laser signal to assure satisfactory communication under all weather conditions;
- sufficiently weak laser signal to assure a margin of safety to the eye at all times;
- operability under all traffic conditions with no cross-talk or interference between communication links.

Initial factors to be considered for each of these issues are established here. They will, of necessity, be considered all at the same time.

1) The received signal strength varies with car movement, and weather condition:

$$I_r = \frac{A}{d^2} e^{-\gamma d} \qquad (1)$$

where A is a constant, d is the distance between transmitting and receiving laser, and γ is an attenuation constant for light passage in the atmosphere. The exponential factor $e^{-\gamma d}$ is referred to as transmittance.

The water droplets in rain or fog retain their spherical shape because of surface tension. Houghton and Walker [5] give an expression of the scattering coefficient as

$$\gamma = \pi \sum_i n_i K_i r_i^2 \qquad (2)$$

where r_i and n_i are the radius and number of particles of the i-th kind per cubic centimeter, and K_i is a scattering area ratio depending on the ratio r_i/λ, λ being the light wave-length. K_i has a peak value of 3.8 and settles down to 2 for $r_i/\lambda >> 1$. Equations (1) and (2) are good for predicting the transmittance in both rain and fog.

For a heavy fog with 200 particles of radius 5μ per cubic centimeter, the coefficient γ at 1μ wavelength is calculated from (2) to be 3.14×10^{-4} cm^{-1}. Using Laws and Parson's rainfall droplets size distribution data [6], Hudson [7] computed the γ -coefficient for a heavy downpour (4 in/hr) to be 5.234×10^{-6} cm^{-1}. The γ -coefficient for snow is difficult to predict because of its irregular particle shape. However, from our own visual experience, a heavy snow is easier to see through than a heavy fog. If we define a transmittance of 0.1 as the extent of visibility, then the visibility for heavy rain and heavy fog are 4390 and 73 meters respectively. The visibility for snow is somewhere in between.

2) The most vulnerable human organ to laser exposure is the eye. An accepted safety standard [8], [9] for the infrared region ($\lambda > 1\mu$) is given below:

(i) Pulses: $5.0\ \mu$J/cm^2 for 1 ns to 50μs.

(ii)Cw & Pulses 5 mW/cm^2 for 10 sec.

We intend to provide a margin of safety below the above mentioned standard.

3) Noise due to various factors, e.g. spontaneous emission, thermal noise, and quantum mechanical uncertainty, in a semiconductor laser light amplifier has been investigated by many authors. [10], [11], [12]. Correlating theoretical and experimental results, Marcuse gives the result that the noise power output N(J) is no more than a few times the quantum mechanical lower noise power limit N_i, where

$$N_i = (G-1)hf\Delta f \qquad (3)$$

where G is the amplifier gain, f and Δf are the lightwave central frequency and bandwidth respectively, and h is Planck's constant.

3.2 COMMUNICATION SYSTEM

The above conditions can be satisfied by a binary digital communication system with error detection and request for retransmission. This kind of system has the advantages of: high reliability in a channel with large variations in signal

strength; and easy implementation with simple and rugged coding and decoding software.

One disadvantage, however, is the requirement for a feedback channel from the receiver to the sender to make the requests for retransmission as needed. This is not a problem for this particular system since two-way communication channels are required for the planned highway system application anyway.

Let us select the following two limiting conditions:

- At the weakest signal level, one Megabyte of information can be transmitted during each pass; and
- At the strongest signal level, laser irradiation stays below 1mW/sec (we note that this gives a 7dB safety margin, the laser energy per pulse is much less than $1\,\mu$J/cm^2 since the number of binary pulses is at least 8 x 10^6 per second in order to transmit 10^6 bytes -one Megabyte- of information).

3.2.1 Nomenclature

A_w : receiver window area.

I : laser beam intensity at the receiver window.

I_p : information transmitted per pass.

F_n : noise factor.

N : laser light amplifier output noise power.

N_i : lower limit on output noise power.

n_b : number of binary bits transmitted per second.

p_e : digit error probability.

p_b : blackout undetected code word error probability.

p_c : probability of correct transmission of a code word.

p_u : undetected code word error probability.

S : laser light amplifier output signal power.

T_p : time for information transmission.

η_c coding efficiency.

η_f filter bandwidth efficiency.

η_o receiving optical system efficiency.

3.2.2 Coding

A m x n matrix parity check code will be used for illustrating the design concept. The matrix elements M_{ij} take on values of 0 or 1. The elements

$i = 1,2,\ldots m\text{-}1, \quad j = 1,2,\ldots n\text{-}1;$

are the message bits, while the elements M_{mj}, and M_{in} are parity check bits:

$$\sum_{i=1}^{i=m} M_{ij} = 0$$
$$\sum_{j=1}^{j=n} M_{ij} = 0 \qquad (4)$$

where Σ denotes modulo 2 sum.

The code detects all code word errors with three or less erroneously transmitted digits. The probability p_u of making an undetectable 4-digit error is

$$p_u = \frac{m(m-1)n(n-1)}{4} p_e{}^4 (1-p_e)^{mn-4} \qquad (5)$$

The probability of correct transmission of a code word is

$$p_c = (1-p_e)^{mn} \qquad (6)$$

There is a fail-safe capability in the retransmission system. Suppose one of the laser lens is covered by condensation, and all information is lost: $p_e = 0.5$. The probability of an undetected error is

$$p_b = 2^{-(m+n-1)} \qquad (7)$$

where $m+n-1$ is the number of parity checks that has to be satisfied by an undetected black-out word error.

With each correctly transmitted coded word b_{id} bits are needed for identification. The code efficiency is

$$\eta_c = \frac{(m-1)(n-1)-b_{id}}{mn} \qquad (8)$$

The information transmitted per pass is

$$I_p = n_b T_p p_c \eta_c / 8 bytes / \sec \qquad (9)$$

where T_p is the time for transmission of information in each pass of the ITS terminal.

Example 1

The following design parameters are assumed: n_b = 10^8/sec., T_p = 0.2 sec., m = 13, n = 14, b_{id} = 12, and $p_e = 5 \times 10^{-4}$.

Then

$$p_u = 4.06x10^{-10}$$

$$p_c = 0.913$$

$$p_b = 1.49x10^{-8}$$

$$n_c = 0.791$$

$$I_p = 1.8x10^6 bytes$$

There are 18 bytes in each code word, the probability of complete correct transmission of 10^6 bytes is 0.99995. During a blackout, the small value of p_b assures that practically every transmitted code word is detected to be in error. During such periods, the entire received message is thrown out.

Assuming that the matrix elements are transmitted row by row, a cyclic distribution circuit plus n+m *exclusive or* circuits constitute all the hardware needed for both coding and decoding. Since the *exclusive or* circuits operate much faster than any single machine instruction, the added cost in time is negligible.

Example 2

For an amplitude modulated binary pulse, p_c can be calculated as:

$$p_e \le \exp\left(-\frac{S}{2N}\right) \qquad (10)$$

Thus the minimum *S/N* to give the assumed p_e is

$$\frac{S}{N} = -2 \ln p_e = 15.2$$

3.2.3 Optical Communication

A two dimensional fixed lens is used to match the laser and laser light amplifiers to open space. The laser beams are controlled along the horizontal direction with their output power concentrated at the opposing terminal. In a car, the LOOC terminal is placed sufficiently away to the right, so that the residue laser light incident upon its passengers is much less. However, we restrict the laser light intensity I at the receiver lens to be within the safety limit as an added protection.

The signal power at the output of the laser light amplifier is

$$S = IA_w\eta_o G$$

where A_W is the window area, η_O is the optical efficiency, and G is the amplifier gain. The signal to noise ratio at the output of the laser light amplifier is then

$$\frac{S}{N} = \left(\frac{G}{G-1}\right)\frac{IA_w\eta_o}{F_n hf\Delta f} \qquad (11)$$

Shannonís sampling theorem gives a pulse rate of $n_b = 2\Delta f$. However, in practical applications the pulse rate is lower by a factor η_f . Thus (11) becomes

$$\frac{S}{N} = \left(\frac{G}{G-1}\right)\frac{2\eta_f\eta_o IA_w}{F_n hf\eta_b} \qquad (12)$$

Example 3

The following design parameters are assumed:

$$\frac{S}{N} = 15.2,\ \eta_f = 0.25,\ \eta_o = 0.01,$$

$$A_w = 20cm^2,\ F_n = 10,\ f = 3x10^{14}$$

and n_b is the same as given in Example 1. Determine I.

Equation (12) gives $I = 3.04 \times 10^{-8}$ watt/cm^2, which is the required minimum I ($I_{\min}$).

3.2.4 Operability

We assume that the HWT is mounted towards the right side of each traffic lane facing on-coming traffic and a VT is mounted on the right side of each vehicle. The vehicles are given the instruction to proceed at a normal speed of 90 to 100 kilometers per hour. If the vehicle intends to communicate with the highway system, it should keep a distance of at least 15 meters from the vehicle ahead. Communication starts when the vehicle is 15 meters from the HWT, and ends when the vehicle is 5 meters from the HWT (measured horizontally). The time allowed for communication is

$$T_p = \frac{(15-5)x3600}{100,000} = 0.36\text{sec}$$

Since it takes less then 0.01 sec for the laser beams to search out each other and lock in, the 0.36 sec period is more than adequate.

In bad weather, the vehicles proceed slowly following safe driving practice and more time is available for communication. However, the extra time is not necessary.

We assume that the transmitted laser power remains constant independent of the weather and traffic conditions. $I_{\min}$ occurs when the vehicle is at a distance of 15m from HWT under heavy fog, and $I_{\max}$ occurs when the vehicle is at a distance of 5m from HWT in clear weather. At closer range, the vehicle is assumed to be shielded from the HWT. Then,

$$\frac{I_{\max}}{I_{\min}} = \left(\frac{15}{5}\right)^2 e^{1500\gamma} = 14.4$$

where $\gamma = 3.14 \times 10^{-4}\text{cm}^{-1}$ is the scattering constant under heavy fog. Thus

$$I_{\max} = 14.4x3.04x10^{-5} mW/cm^2 \qquad (13)$$

$$= 4.4x10^{-4} mW/cm^2$$

It is ten thousand times weaker than the allowed maximum of 5mW/cm^2.

Figure 3 gives the computed digit error probability, p_e, undetected code word error probability, p_u, and retransmission probability, p_r, respectively. The y-axis is numbered in terms of exponentially descending order of probabilities. If we choose 10^{-9} (one in a billion) as the boundary of improbability, we notice that in all cases an undetected error is beyond this limit. As the vehicle moves close to HWT, even retransmission becomes improbable.

3.2.5 Signal Interference

There is no interference under heavy traffic conditions because both HWT and VT laser beams are sharply directed towards their opposing terminals, the receiving lasers are also direction controlled. Multiple reflected wave energies are much too small to change the outcome of a binary pulse.

3.3 AUTOMATED HIGHWAY SYSTEM

On the highway side the only installations are the reflectors on the lane dividing lines as shown in Figure 2. The active sensing, speed and steering control work is completely done at the vehicle terminal. As shown in Figure 2, there is one DAFL on each side of the front end of the vehicle for sensing the position of the reflectors and one DAFL in front for sensing the position and speed of any obstacle ahead. Each reflector sensor determines the reflector direction by equalizing the average reflected pulse strengths in the two receiving lobes, and distance is determined by measuring the time delay of the reflected pulses. The obstacle sensor works in the same way as an ordinary radar, and scans electronically across the road ahead. With sharp lightwave pulses it makes accurate determination of both the obstacle's position and its velocity.

3.3.1 Reflector Sensing Signals and Steering Control Law

Reflectors are arranged in pairs on the two lane dividing lines, such that the straight line joining each pair of reflectors is perpendicular to the lane's direction. The center of the joining line will be referred to as a reference point. As the vehicle moves forward, the DAFL beams automatically switches to pairs of reflectors at a certain distance range in front. The vehicle distance u is measured as the arc length along the center line of the lane from a given point. In a straight section of the highway, u is the straight line distance. There is a *window range* w_i in which the DAFL beams aim at the pair of reflectors at reference point u_i:

$$w_i : u_i - u_2 \le u \le u_i - u_1 \qquad (14)$$

Let θ and V denote the direction and speed of vehicle motion, and θ_i denote the direction of the reference point at u_i relative to the vehicle, a simple steering control law is

$$\frac{d\theta}{dt} = \frac{1}{\tau}(\theta_i - \theta) \qquad (15)$$

The time constant τ can be a constant or a known function of time.

3.3.2 Analysis

Let $a = u_i - u$, r_o denote the lane's radius of curvature, r_1 denote the vehicle's shift from the center line of the lane, and θ_1 denote the lane directional angle. Let $\beta = \theta - \theta_1$ and $\beta_i = \theta_i - \theta_1$. Under highway driving conditions, $r_1 << a << r_o$ and both β and β_i are small angles. The following equations are in first order approximation:

$$\frac{dr_1}{dt} = -V\beta \qquad (16)$$

$$\beta_i = \frac{a}{2r_o} + \frac{r_1}{a} \qquad (17)$$

$$\frac{d\theta_1}{dt} = \frac{V}{r_o + r_1} = \frac{V}{r_o} - \frac{Vr_1}{r_o^2} \qquad (18)$$

substituting (17) and (18) into (15) gives

$$\frac{d\beta}{dt} = \frac{1}{\tau}\left(\frac{a}{2r_o} + \frac{r_1}{a} - \beta\right) - \frac{V}{r_o} + \frac{Vr_1}{r_o^2} \qquad (19)$$

Equations (16) and (19) are state equations of the error variables β and r_1. The expression

$$E = \frac{1}{\tau}\cdot\frac{a}{2r_o} - \frac{V}{r_o} \qquad (20)$$

in (19) represents an input to errors β and r_1. Setting $E = 0$ gives

$$\tau = \frac{a}{2V} \qquad (21)$$

Since both a and V are known quantities, the control law (15) supplemented by (21) is readily implemented with computer firm-ware. The stability of the control law is to be analyzed. Since $du = Vdt$, (16) and (19) can be rewritten as

$$\frac{dr_1}{du} = -\beta \qquad (22)$$

$$\frac{d\beta}{du} = \left(\frac{2}{a^2} + \frac{1}{r_o^2}\right) r_1 - \frac{2\beta}{a} \qquad (23)$$

and a is a saw tooth function of u. Computer simulated results show that the system is stable. Initial values of r_1 and β reduce to zero as u increases. In deriving (22) and (23), we did not assume that V is constant. The stability of the system is thus invariant to vehicle speed variations.

In the simulation, we assume that the center of the reflectors are equally spaced at a distance U apart;

$$u_n = nU, \qquad n = 1,2 \ldots \qquad (24)$$

Then a is a sawtooth function of u with periodicity U. Numerical integration of one period is sufficient to give the 2x2 matrix function $A\ (u, u')$ defined by

$$\begin{pmatrix} r_1 & (u) \\ \beta & (u) \end{pmatrix} = A(u,u')\begin{pmatrix} r_1 & (u') \\ \beta & (u') \end{pmatrix} \qquad (25)$$

For instance, if $u' = 0$, and $u = nU + u''$, then

$$A(u,0) = A(u'',0)A(U,0)^n \qquad (26)$$

Example 4

In an AHS, the reflectors are placed at equal distances of $U = 5m$ apart along each side. The reflector searching lasers are programmed to beam at the third reflectors. Then $u_1 = 10m$ and $u_2 = 15m$. Determine the A matrix, and system stability.

Solution

For each period of $0 \le u \le 5$.

$$a = 15 - u \qquad (27)$$

Numerical solution of (22), (23), and (27) gives the matrix elements A_{ij} of Table 1,

Table 1

r_0	A_{11}	A_{12}	A_{21}	A_{22}
100	0.887926	-3.332333	0.044747	0.332528
200	0.888620	-3.333375	0.044524	0.333049
300	0.888749	-3.333568	0.044483	0.333145
∝	0.888852	-3.333722	0.044450	0.333220

where $A_{ij}=A_{ij}(5,0)$ for $i = 1, 2$; and $j = 1,2$. We note that within the normal range of highway curvatures, the matrix elements do not change much. The system stability can be determined by finding the roots of z in the equation.

$$(z-A_{11})(z-A_{22})-A_{12}A_{21}=0 \qquad (28)$$

If $|z|>1$, the system is unstable. Equation (28) gives $|z|<0.67$ in all four cases. Thus the system is very stable.

In the above example, the control time constant τ is required to vary with a according to (27). An alternative is to use the average value of $\bar{a} = 12.5$ in (21). Then there is a non-homogeneous or residue term E in (19); and

$$\begin{pmatrix} r^1 & (5) \\ \beta & (5) \end{pmatrix} = A(5.0)\begin{pmatrix} r^1 & (0) \\ \beta & (0) \end{pmatrix} + \begin{pmatrix} \hat{r}_1 \\ \hat{\beta} \end{pmatrix} \qquad (29)$$

where $\hat{r}_1$ and $\hat{\beta}$ are errors due to E of (20). Table 2 gives the computed values of $A(5,0)$, $\hat{r}_1$ and $\hat{\beta}$. The A values in Table 2 are very close to that in Table 1. The errors r_1 and β are due to the non-vanishing E term in (20). They are very small.

Table 2

r_0	A_{11}	A_{12}	A_{21}	A_{22}
100	0.883134	-3.260484	0.043790	0.347036
200	0.883829	-3.261515	0.043560	0.347564
300	0.883958	-3.261706	0.043517	0.347661
∝	0.884061	-3.261859	0.044450	0.347740

r_0	$\hat{r}_1$	$\hat{\beta}$
100	-0.005388	-0.001090
200	-0.002695	-0.000545
300	-0.001797	-0.000363
∝	0.000000	0.000000

3.3.3 Simulation Study on a Typical Highway

Figure 4(a), (b), (c), and (d) illustrate the results of a simulation study on a typical highway. Figure 4(a) gives the *x-y* plot of the center line of a typical highway which starts with a *100m* straight line section and then follows the description below:

- For the next *100m*, the curvature changes linearly from 0 to *1/200* m^{-1}.
- For the next *100m*, the road turns at a constant radians of *200m*.
- For the next *100m*, the curvature changes linearly from *1/200* m^{-1} to *-1/300*m^{-1}.
- For the next *100m*, the road turns the other way at a constant radius of *300m*.
- For the next *100m*, the curvature changes back to 0.

Figure 4(b) gives the position error versus distance with an initial position error of *1m*. Figure 4(c) gives the position error versus distance with an initial heading error of *0.1* radian. Both (b) and (c) illustrate deterministic results, and the position error reduces to zero after traveling a short distance. Figure 4(d) illustrates the case of a random heading error of approximately *0.2m* away from the center position for each pair of reflectors. The direction of error for successive pairs of reflectors are uncorrelated. The random heading error induces a random lateral shift of the vehicle. The induced lateral shift is well within tolerable limits.

3.3.4 Reflected Light Signals

In studying the reflected light signal we assume that the highway is one directional. The opposite traffic is either far away or screened off by a central divider.

Figure 5 illustrates a cross-section of the reflected light geometry in the plane OPP' where, P is the position of the light source. P' is a point in the reflected light beam, and 0 is the center of the reflector. R is its radius. Q and Q' are points on the surface of the reflector. A, B, C, and L are angles as illustrated.

Let d denote the distance PQ. Some general relations are given below:

$$\frac{\sin A}{R} = \frac{\sin B}{PQ'} \tag{30}$$

$$C = A + B \tag{31}$$

$$2C = L + A \tag{32}$$

From (31) and (32)

$$L = 2C - A = 2B + A \tag{33}$$

Let I_i denote the incident light intensity at the reflector surface, and I_r denote the reflected light intensity at P. To calculate I_r, we make $A \to 0$. Consequently all the angles B, C, and L approach 0, and $PQ' \to d$. Consider a light cone PQ' about axis PQ and its reflected light cone $O'P'$ about the same axis. The incident and reflected light energies are

$$E_i = \pi(dA)^2 I_i \tag{34}$$

$$E_r = \pi(d' L)^2 I_r \tag{35}$$

where d' is the distance $0'P$. Let η denote the coefficient of reflection: $\eta = E_r / E_i$. Then

$$I_r = \left(\frac{dA}{d' L}\right)^2 \eta I_i \tag{36}$$

From Figure 5

$$\frac{d}{d'} = \frac{\sin L}{\sin 2C} = \frac{L}{2C} \tag{37}$$

Substituting (37) into (36) gives

$$I_r = \left[\frac{R}{2(R+d)}\right]^2 \eta I_i \qquad (38)$$

3.3.5 AHS Design

Three items are to be discussed in this section: reflector design, light pulse design, and light noise elimination.

3.3.5.1 Reflector Design

The reflector sensing lasers are placed approximately *0.5m* above ground. consequently the active part of each reflector is no more than *0.1m* above ground. Its top above *0.1m* is flattened so that if a vehicle strayed and ran over a reflector, it would not result in an accident.

3.3.5.2 Light-Pulse

The width T of the light pulse introduces a distance uncertainty $\cong 0.5cT$. It can be much reduced by utilizing the rising edge of the pulse. However, to utilize the rising edge would require a larger S/N and a larger bandwidth than the minimum value [13] of 1/T. The following illustrates such a design.

Example 5

$T = 2x10^{-10}$ sec

$\Delta f =$ amplifier bandwidth = $2 \times 10^{10} hertz$

$$\frac{S}{N} = 100$$

$f = 2x10^{14}$ *hertz*

Determine the light intensity, number of light pulses per second, and random noise reduction [14] factor:

Solution

Equation (11) gives the reflected intensity

$I_r = 1.325x10^{-5} watt / cm^2$

The incident light energy per pulse is

$$E = TI_i = 2x10^{-10} x\left(\frac{I_i}{I_r}\right) I_r$$

$$= 2x10^{-10} x2.89x10^4 x1.325x10^{-5}$$

$$= 7.66x10^{-11} J / cm^2 = 7.66x10^{-5} \mu J / cm^2$$

Let n_p denote the number of pulses per second. There are two safety criteria one is on the light energy per pulse, while the other is on the average intensity. We choose n_p to satisfy both by the same margin:

$$n_p = 1000 \qquad (39)$$

Then the average incident light intensity is

$I_a = 1000E = 7.66x10^{-5} mW / cm^2$

Both the energy per pulse, and average light intensity are more than 40dB below the accepted safety standard.

Using the data of Example 4 and a vehicle speed of 30m/sec, the number of light pulses impinging on each reflector in one pass of the vehicle is

$$1000x\frac{5}{30} = 166$$

It is a sufficient number to average out the random errors by a factor of

$\sqrt{166} = 12.9$

3.3.5.3 Light noise elimination

There are at least two ways of light noise pulse elimination:

Windowing

Because of the regularity of the reflectors, the arrival time of each reflected pulse can be expected to fall within a time interval *W*. The windowing process is to ignore all the pulses which fall outside of *W*, and to ignore completely the information carried by pulses in W if there are two or more such pulses with amplitudes above an acceptable threshold. There are only a few vehicles and a few reflectors sufficiently close to generate reflected noise pulses with magnitudes above threshold. Since the pulse originating times of different vehicles are not correlated, the noise pulses arrive at random. The blanking probability p_{bk} that one or more noised pulse falls within *W* is

$$p_{bk} = 1 - e^{-WA} \qquad (40)$$

where A is the noise pulse Poisson arrival rate.

Example 6

Let W correspond to a reflector position error of *0.6m*, and $A = 5{,}000$ pulses per second. Determine p_{bk}.

Solution

$$W = \frac{2x0.6}{c} = 0.4x10^{-8}$$

$$WA = 0.4x10^{-8}x5000 = 2x10^{-5}$$

$$p_{bk} = 2x10^{-5} \qquad (41)$$

Missing one reading among fifty thousand is not significant.

Frequency discrimination

Different laser frequencies can be used on different vehicles to reduce p_{bk} For instance, two different laser frequencies can be installed on different cars with the instruction to use only odd (even) numbered AHS lanes if there are more than one lane. This arrangement would eliminate noise pulse generation between adjacent lanes.

3.4 TERMINAL DEVICES

Figure 6 illustrates the vehicle terminal (VT) design. Communication between the driver and VT is through a monitor with input buttons or voice communication, display electronics, and interactive IO logic. The driver's message is processed through the car's CPU and stored in the memory of the store and forward logic. When the vehicle approaches an overhead bridge, the BEAM CONTROL automatically lines up the DAFL receiving direction with the highway system terminal (HWT) transmitting beam and vice versa. The control of the beams are done electronically in microseconds without any moving parts. Error-detection-and-retransmission code is used for signal transmission because of its high reliability. In the event that errors are detected, message retransmission is arranged by sequencing control.

In Figure 6, the functions of interactive IO logic, store and forward, sequencing control, coding decoding (CDC) logic, and beam control are realized by firm ware (read only memory) in the micro-computer. All the firm wares share a common random access memory (RAM) with the CPU. The disk is used to store large blocks of data. For instance road maps can be coded in computer vector graphics and stored on the disk. They are to be displayed with added road condition information on the monitor as needed.

A highway system terminal is very similar to the VT in design. However, the provisions for user interface is replaced by a network communication line to the Traffic Operations Center (TOC) as shown in Figure 7.

Figure 8 illustrates the vehicle terminal device design for the Automated Highway System (AHS). Because the time needed for HWT-VT communication can be easily spared by the vehicle terminal from its AHS functions, the same CPU, monitoring system, RAM, and DISK are time-shared between the two systems. The special computing functions of reflector range finder, beam control, automatic steering control, DAFL radar, and automatic speed control are realized with computer firm ware.

Figure 9 illustrates the transmitting DAFL beam pattern and receiving DAFL sensitivity pattern of two corresponding terminals in the horizontal plane. The radiation patterns are fixed vertically. The receiving DAFL angle is automatically controlled to yield equal signal strength in the two lobes. The transmitting beam pattern and receiving sensitivity patterns for the same side are aligned. Therefore, once communication is established in one direction, it is also established in the other direction.

For AHS the same beam control firm ware is used. However, the opposite transmitting beam is replaced by the reflected beam. The reflector range is determined by the time delay between transmitted and reflected laser pulses. The DAFL radar and steering signals can also be used as a driver's aid in bad weather. In general, the laser's infrared sighting distance is longer than that of the eye. The signals can be used to monitor obstacles ahead and their speeds, and the vehicle's positional deviation from the center of the lane.

Microwave communication devices and GPS can also be added to the vehicle terminal with the same computer. A PC has more than adequate capacity for all the above mentioned functions. With the added devices, but without a keyboard, a vehicle terminal can be mass-produced and sold in the price range of $1,000 to $2,000.

4. RESULTS - AN IDEA PRODUCT

In our proposed IDEA system, a number of HWT's and AHS's are installed at population centers to meet highway communication and automated driving needs. Automatic toll collection, share-ride information, up-to-the-minute general road conditions, "best route" information, motel, gas, shopping, and repair shop information can all be easily transacted during one encounter of the VT with a HWT.

The IDEA-AHS is capable of satisfying many automated driving needs:

. IDEA-AHS is well suited to both urban and rural operational environments;

. Check in and check out operations are as simple as turning on and off the cruise control, assuming that ordinary precautions in switching lanes are observed;

- Longitudinal control is maintained by a signal from the front end DAFL, which gives both the relative speed and position of the vehicle in front, lateral control is maintained by the reflector sensing DAFL signals, which give look-ahead lane guidance;

· IDEA-AHS is easily deployed within existing freeway networks; and

- IDEA-AHS can help relieve congestion from nearly parallel roadways by increasing capacity.

Both the vehicle terminals (VT) and highway system terminals (HWT) are suitable for mass-production. Vehicle terminal sales potential is in the range of millions of units per year. While HWT sales potential is lower in comparison, volume there is also in a respectable range. Standard regional maps in vector graphics are very useful for VT and are commercially available in many areas.

Specific local information and operational programs for HWT can be recorded on disks or diskettes. When a HWT needs to be serviced, its hardware can be replaced by a standard shelf item, and its software can be transferred within minutes. Since a personal computer rarely breaks down, the down time of a HWT would be almost nil.

5. CONCLUSIONS

The main result of the present research is an LOOC product to facilitate ITS implementation.

On the PRO side, development of our IDEA product is a job well suited to private industrial competition. With adequate funding development of our IDEA product will take no more than five years. A fully augmented system's implementation can be achieved within ten years.

On the CON side, we have not yet produced the first DAFL. There is no doubt of DAFL's scientific design feasibility but facilities for development and production of the DAFL may require funding on the order of several million dollars.

Our planned next step is a Phase II research proposal. The proposed project will have three tasks:

. Realization of Phase I IDEA products with a laser having servo-controlled beam direction (LSBD). This is a hardware project for realizing our Phase I IDEA products with LSBD instead of DAFL. The same computer and electronics are used. LSBD can be done with a rugged servo-controlled deflecting mirror design. It is probably more costly and less rugged than the DAFL, but can be used to realize the same goals.

- Further studies on methods of DAFL production. Two methods of modifying a molecular beam epitaxy machine to produce DAFLs will be considered. The proposed study may also include investigation of other fabrication methods.
- Applications of DAFL and LSBD to transportation safety for autos, trains, and possibly aircraft.

REFERENCES

[l] S. Chang. Integrated semiconductor laser with electronic directivity and focusing control. U.S. Patent NO. 5233,623.

[2] ITS Architecture Development Program, Phase I ITS America, November, 1994.

[3] N. Congress. Automated Highway System, An Idea Whose Time Has Come. *Public Roads.* Vol. 58, No. 1, Summer 1994.

[4] L. Saxton. Automated Control-Cornerstone of Future Highway Systems. IVHS Review, Summer 1993, pp. I-16.

[5] H. Houghton and W. Walker. The scattering cross-section of water drops in visible light. J. *Opt. Soc. Am.*, Vol. 39, 1949, p. 955.

[6] J. Laws and D. Parsons. The relation of raindrop size to intensity," *Trans. Am. Geophy. Union, Vol 24, 1943, p.* 452.

[7] R Hudson. *Infra-red Systems Engineering.* John Wiley, New York, 1969, p. 164.

[8] ANSI Standard 2-136.1 - 1986; ACGIH TLVs, 1988; and lRPA, 1988.

[9] D. Sliney and S. Trokel. *Medical Lasers and Their Safe Use.* p. Springer Verlag, 1993, p. 77.

[10] Y. Yamamoto. Noise and error rate performance of semiconductor laser amplifiers in PCM-IM optical transmission system. *IEEEJ. Quantum Electron,* Vol. QE-16, 1980, p. 1073.

[l l] J. Simon. Semiconductor laser amplifier for single mode optical fiber communications. J. *Opt. Comm.,* Vol. 4, 1983, p. 5 1.

[12] D. Marcuse, D. Computer model of an injection laser amplifier. *IEEEJ. Quantum Electron,* Vol. QE-19, 1983, p. 63.

[13] *S.* Chang. *Fundamentals Handbook of Electrical & Computer Engineering* II. John Wiley, New York, 1983, p. 51.

[14] *S.* Chang. *Synthesis of Optimum Control Systems. McGraw Hill, 1961, p. 327.*

[15] 0. Madelung. *Group IV Elements and III-V Compounds.* Springer-Verlag, New York, 199 1.

[16] Parker. *The Physics and Technology of Molecular Beam Epitaxy.* Plenum Publishing, 1985.

[17] J. Moore, C. Davis and M. Coplan. *Building Scientific Apparatus.* Addison-Wesley, 1983, p. 305.

[18] W. Tsang and A. Cho. *Applied Physics Letters.* Vol. 32, 1978, p. 491.

APPENDIX A: DIRECTED AND FOCUSING LASER

The directed and focusing laser can be described as an electronically controlled antenna phase array for the light-waves. Because of the short wave-length, each antenna element is replaced by a phase controlled channel (PCC) for light passage, and the array of PCC's is built on a single semiconductor chip. Thus the building blocks of DAFL are the PCC's and their design is based on the following physical principle: the index of refraction n of a semiconductor is dependent on its carrier density N, and N can be controlled through injected electric current.

The dependence of n on N is expressed as:

$$n = n_o + n_1(N - N_o) \tag{47}$$

where N_O is the transparent carrier density, n_O and n_1 are all complex valued functions of the semiconductor material composition, and lightwave frequency ω.

The complex valued n_1 can be expressed as

$$n_1 = n_r + in_i \tag{48}$$

where n_r and n_i are both real. A positive n_r represents an increase in the index of refraction as N increases. A positive n_i represents stimulated emission.

A.1 DETERMINATION OF N_R AND N_I

The coefficients n_r and n_i are functions of light frequency, semiconductor material composition, N_O, and temperature T. Their values are needed for DAFL design. But in the open literature, there is nothing on their measurements nor a theory to predict their values. Our approach is to develop a mathematical model on n_i and n_r first, and then spot check the theoretical results with measurements.

Using the density matrix method in quantum mechanics, the complex susceptibility $\chi(\omega, N)$ of a semiconductor with direct energy gap can be written as

$$\chi(\omega, N) = \int_0^\infty \rho(\omega_1)\left[f_c(\omega_1) - f_v(\omega_1)\right] S(\omega, \omega_1) d\omega_1 \tag{49}$$

where $\rho(\omega_1)$ is the density of states at transition energy $\hbar\omega_1$, f_C and f_V are Fermi distribution functions, $f_C(\omega_1)$ - $f_V(\omega_1)$ is the net probability that an electron in the conduction band can be transferred to fill a corresponding hole in the valence band, and $S(\omega, \omega_1)$ is the contribution to $\chi(\omega, N)$ by each transferable electron. For $\chi(\omega, N) << 1$, the index of refraction n is related to $\chi(\omega, N)$ by

$$n = n_o\left[1 + \frac{1}{n_o^2}\chi(\omega, N)\right]^{1/2} = n_o + \frac{1}{2n_o}\cdot\chi(\omega, N) \tag{50}$$

From (47) and (50)

$$n_1 = \frac{1}{2n_o}\left[\frac{d\chi(\omega, N)}{dN}\right]_{N=N_o} \tag{51}$$

For sufficiently small ω_1

$$\rho(\omega_1) = \frac{1}{2\pi^2}\left(\frac{2m_r}{\hbar}\right)^{3/2}\omega_1^{1/2} \tag{52}$$

Since transitions between bands are far less frequent than collisions between particles in the same band, it can be assumed that approximate equilibrium states exist separately in the conduction and valence bands respectively;

$$f_c(\omega_1, N)=\left[1+\exp\left\{(A_c\hbar\omega_1 - E_{Fc})/kT\right\}\right]^{-1} \quad (53)$$

$$f_v(\omega_1, N)=\left[1+\exp\left\{(-A_v\hbar\omega_1 + E_{Fv})/kT\right\}\right]^{-1} \quad (54)$$

where $A_C = m_r/m_C$; $A_V = m_r/m_V$; m_C, m_V and m_r are the effective mass of electrons in the conduction band, density of state effective mass of holes [15] in the valence band, and the relative mass respectively. Since

$$\frac{1}{m_r} = \frac{1}{m_c} + \frac{1}{m_v} \quad (55)$$

it follows that $A_c + A_v = 1$. E_{FC} and E_{FV}- are the Fermi energies measured from the lowest point in the conduction band, and highest point in the valence band respectively. In an intrinsic semiconductor compound, the density of electrons in the conduction band, and the density of holes in the valence band are both equal to the injected carrier density N. Therefore

$$\int_0^\infty \rho(\omega_1) f_c(\omega_1) d\omega_1 = \int_0^\infty \rho(\omega_1)\left[1-f_v(\omega_1)\right] d\omega_1 = N \quad (56)$$

Equation (56) can be used to determine E_{FC} and E_{FV} Using the density matrix method, $S(\omega, \omega_1)$ is derived as

$$S(\omega, \omega_1)=\frac{i\mu^2 T_2}{\varepsilon_0\hbar}\left(\frac{1}{1+iT_2(\omega-\omega_1-E_g/\hbar)}\right) \quad (57)$$

In (57) μ is a characteristic dipole moment, and T_2 is a relaxation time constant for the off-diagonal element of the density matrix. Equation (57) is derived under the assumption that ω is close to the resonant frequency ω_0 where $\omega_0 = \omega_1 + E_g/\hbar$.

Equations (49) to (57)) inclusive can be used to compute n_1. Fig. 10 gives the computed result for the semiconductor material $Ga_{.95}Al_{.05}As$ in dimensionless form:

$$C(\omega, N)=\left(\frac{2n_o\varepsilon_o kT}{\mu^2}\right) n_1(\omega, N) \quad (58)$$

$$x=(\hbar\omega - E_g)/kT \quad (59)$$

From Fig. 10, the following design significant results are obtained:

1. The positive and negative peaks of n_r occur at $\omega_p \pm \frac{2kT}{\hbar}$ where ω_p is the lightwave frequency in radians per second at peak gain.

2. The maximum change in n_r (as x varies) is larger than the peak value of n_i.

A.2 DAFL DESIGN

A.2.1 Phase controlled channel (PCC)

Each PCC is an isolated path for light-waves. The phase delay along each PCC can be expressed as

$$\phi = \frac{\omega_o}{c}\int_0^L n(y)dy \quad (60)$$

The energy gap E_g of the semiconductor $Ga_{1-q}Al_qAs$ is a function of q:

$$E_g = (1.424 + 1.266q)eV \quad (61)$$

Along each PCC, the value of q varies with the length variable y. Consequently ω_p is a function of y. Referring to Fig 10, (47), and (58), the index of refraction n is a function of ω_p(y) and the injection current J(y). Therefore

$$n(y) = n(\omega_p(y), J(y)) \qquad (62)$$

The phase delay ϕ along a PCC is increased by increasing J(y) at places where $\omega_p < \omega_0$, and decreasing J(y) otherwise, and ϕ is decreased by doing the opposite. Thus the injection current distribution J(y) can be used to control ϕ.

Equations (60), (61), and Fig. 10 constitutes the basis for phase controlled channel design.

A.2.2 PCC Array

The directed and focusing laser can be designed as an array of phase controlled channels. Referring to Fig. 11, ϑ is an angle from the forward y-direction; d is the channel spacing along the x-direction; and m is the total number of channels. Since md < 0.001 m, and the minimum distance of interest is 5 m, far zone approximation can be used. Let $E(\vartheta)$ denote the lightwave electric field intensity pattern of each channel at an angle ϑ, A_n and ϕ_n denote the amplitude and phase delay of the n-th channel. Then the total field intensity at ϑ can be expressed as

$$F(\vartheta) = \sum_{n=0}^{n=m-1} A_n E(\vartheta) \exp\{j(nkd\sin\vartheta - \phi_n)\} \qquad (63)$$

where $k = 2\pi/\lambda$. To have peak intensity at ϑ_1, (63) gives

$$\phi_n = nkd\sin\vartheta_1 + 2\pi N \qquad (64)$$

where N is an integer. It can be selected so that the required phase-shift $|\phi_n|$ in any channel is no more than π. This result implies that the required length of each PCC is approximately that of a high gain traveling wave amplifier of the same material.

Let $\psi = kd(\sin\vartheta - \sin\vartheta_1)$. For the special case of A_n = 1, (63) gives

$$F(\vartheta) = \left[\frac{\sin(m\psi/2)}{\sin(\psi/2)}\right] \exp\{j(m-1)\psi/2\} E(\vartheta) \qquad (65)$$

The exponential multiplier is immaterial to beam intensity. For $\vartheta \cong \vartheta_1$

$$\begin{aligned} \psi &= 2kd\cos\frac{1}{2}(\vartheta + \vartheta_1)\sin\frac{1}{2}(\vartheta - \vartheta_1) \\ &\cong kd(\vartheta - \vartheta_1)\cos\vartheta_1 \end{aligned} \qquad (66)$$

The beam width is obtained by setting

$$m\psi = \pm\pi \qquad (67)$$

It gives

$$\vartheta_\pm = \vartheta_1 \pm \frac{\pi}{mkd\cos\vartheta_1} \qquad (68)$$

The beam width in radians is

$$\Delta\vartheta = \vartheta_+ - \vartheta_- = \frac{\lambda}{md\cos\vartheta_1} \qquad (69)$$

At $\vartheta = \vartheta_\pm$, the beam intensity is reduced to 0.4 of its peak value. With A_n = 1, (65) shows that side lobes of radiation can occur at

$$\psi_s = (2N+1)\pi/m \qquad (70)$$

where N is an integer. These side lobes can be significantly reduced by choosing appropriate values for A_n. However, aliasing can occur at

$$\psi_a = 2N\pi \qquad (71)$$

with the ratio $F(\vartheta)/E(\vartheta)$ equal to the same ratio at the main peak. Aliasing can be avoided by shaping $E(\vartheta)$ or choosing $d \leq \lambda / 2$.

A.2.3 An example of DAFL design

The beam widths of the transmitting and receiving DAFL's are set at 0.05 and 0.1 radian respectively. The maximum angle of deflection is ± 0.3 radian. Determine the number of phase controlled channels for each.

Solution Let $d = 0.5\lambda$ Equation (69) gives

$$m = \frac{2}{\Delta\vartheta \cos\vartheta_1}$$

The answer is 41 PCC's for the transmitting DAFL, and 20 PCC's for the receiving DAFL. Because the information bandwidth is much smaller than the light-wave frequency, a maximum controlled phase change of 2π is adequate for each channel. It can be realized with a channel length less than 1mm.

A.2.4 Number of available infra-red communication channels

From the lightwave frequency response curves of Fig. 10, a channel separation of $6kT \cong 0.15eV$ is adequate. The two III-V alloy compounds GaAlAs, and GaInAsP cover a gap energy range from 0.66 eV to 2.16 eV. The number of available communication channels is

$$N_{CH} = \frac{2 \cdot 16 - 0.66}{0.15} = 10$$

A.3 DAFL PRODUCTION

A DAFL phase controlled channel is very similar to a double hetero-structure $Al_qGa_{1-q}As$ laser in design. The laser's semiconductor wave guide can be grown in a molecular beam epitaxy (MBE) machine. But the same MBE machine can not be used to produce the DAFL phase controlled channel (PCC) for the following reason: The q-value is constant throughout the laser wave-guide, but varies by as much as 0.08 periodically in a DAFL PCC along the direction of light propagation.

Fig. 12 is a schematic diagram of the MBE process for the growth of p-and n-type $Al_qGa_{1-q}As$ [16]. Fig 12 itself is parallel to the x-y plane. The GaAs waver surface is parallel to the x-z plane. The crystal growth is in the -y direction, and lightwave propagation in the finished product is along the z-direction. In general the growth rate is low - around 1 μm /hour or / monolayer / second. For both the laser waveguide and the DAFL PCC the growth thickness is generally a fraction of a μm.

To grow the laser waveguide the beam intensities of all five materials are maintained at constant values throughout the process. To grow DAFL, the Al and Ga molecular beams are required to vary periodically by a specified small amount along the z-direction. We are investigating two ways of doing this:

1. *Using Al and Ga molecular ion sources* [17]. The periodic beam intensity spatial variations are then realized with electrostatic diffraction.

2. Using periodically varying molecular beam intensities and synchronized mask movements along the z-direction. The moving mask idea and experimental results were reported in [18].

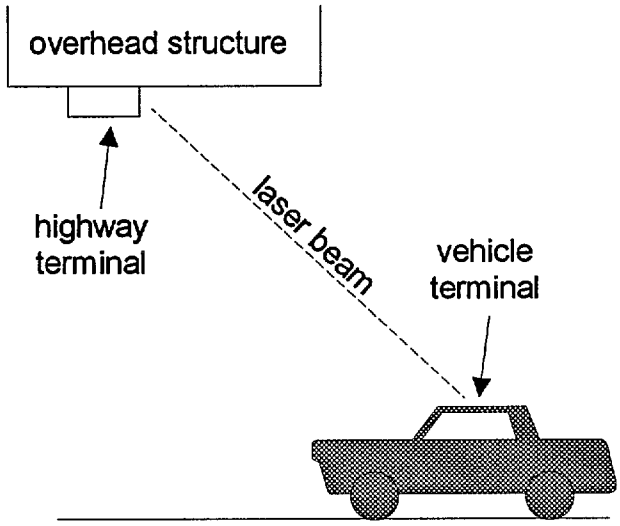

FIGURE 1 Communications between vehicle and highway system terminals.

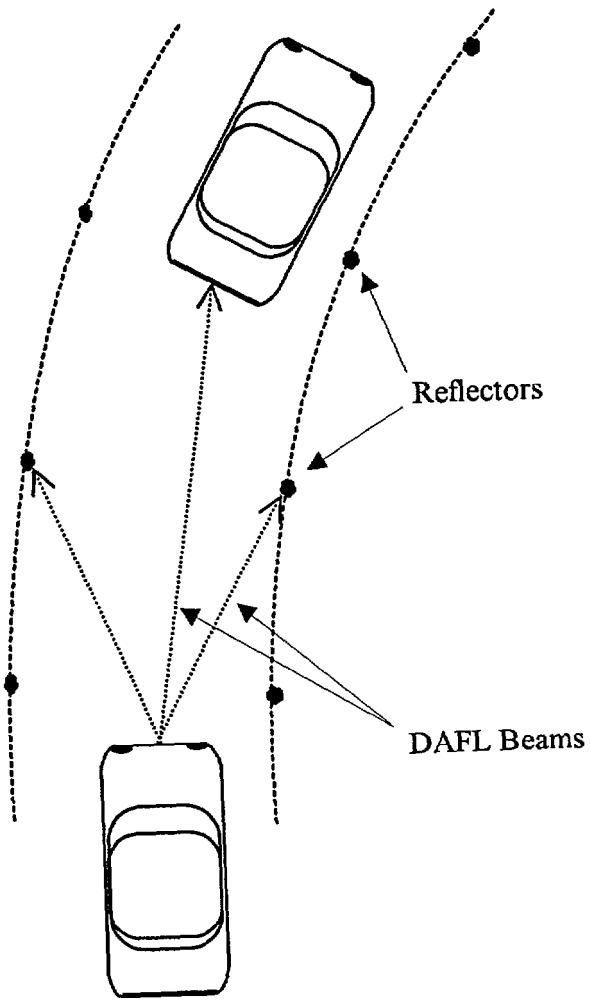

FIGURE 2 Use of DAFL in automated highway systems.

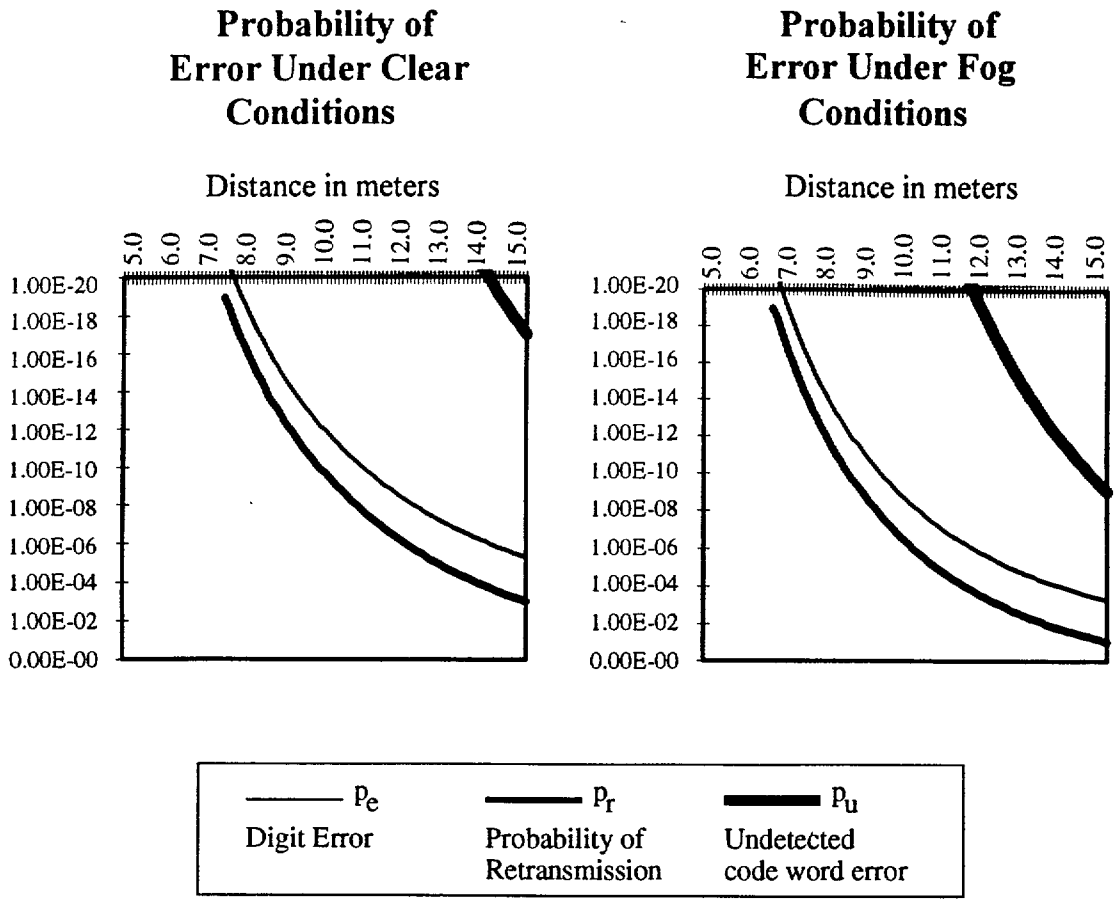

Fig. 3 Probabilities of error versus vehicle distance

Fig. 4 (a)

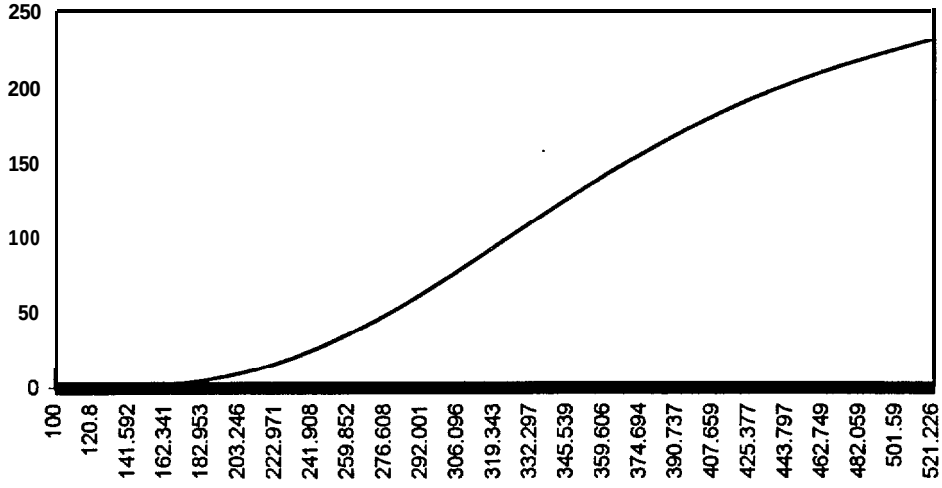
250
200
150
100
50
0
100
120.8
141.592
162.341
182.953
203.246
222.971
241.908
259.852
276.608
292.001
306.096
319.343
332.297
345.539
359.606
374.694
390.737
407.659
425.377
443.797
462.749
482.059
501.59
521.226

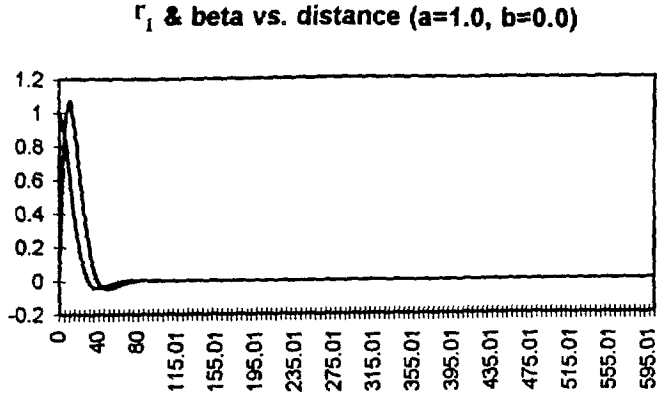

(b) lateral position error from lane center line and heading error versus distance with initial position error.

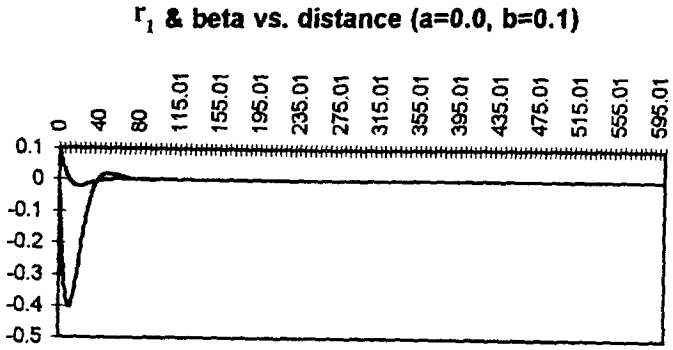

(c) same as (b) with initial heading error

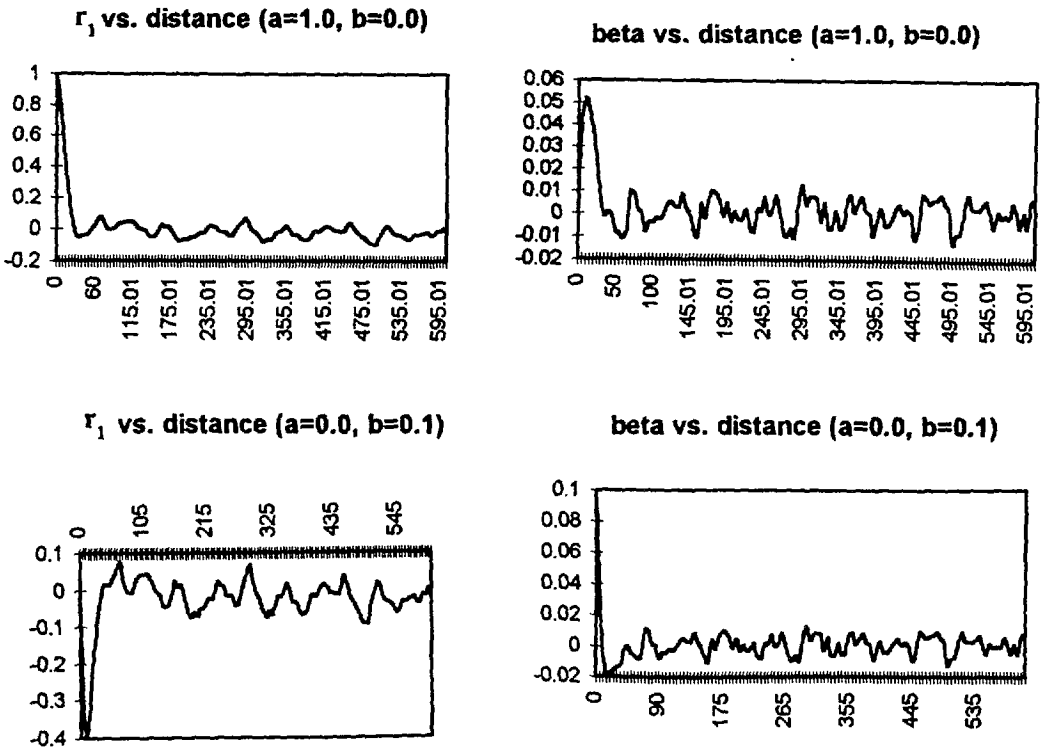

(d) effects of random error in measured direction of reference points. All units are in meters and radian respectively.

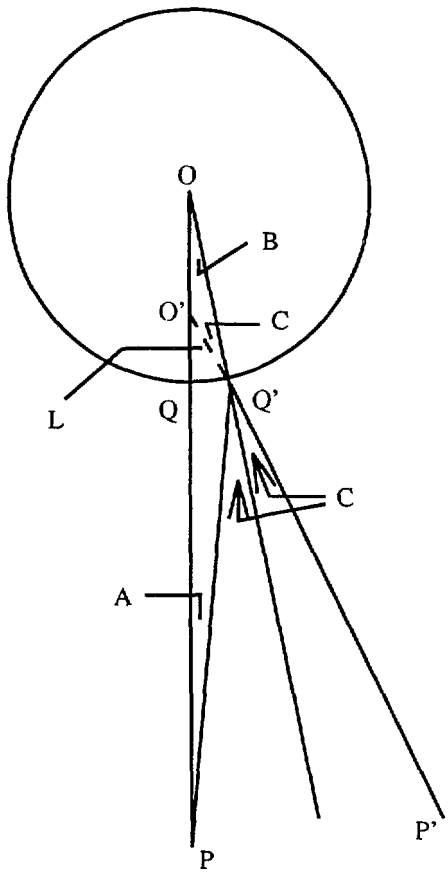

Fig. 5 Across-section of the light-reflecting geometry

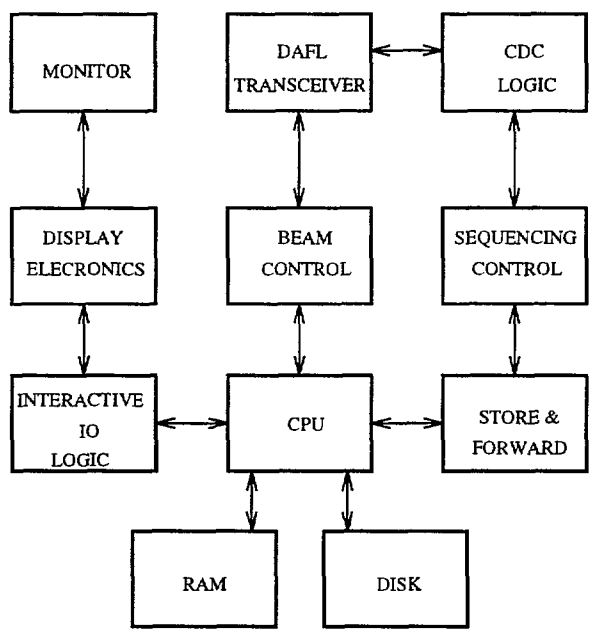

Fig. 6 Vehicle terminal design

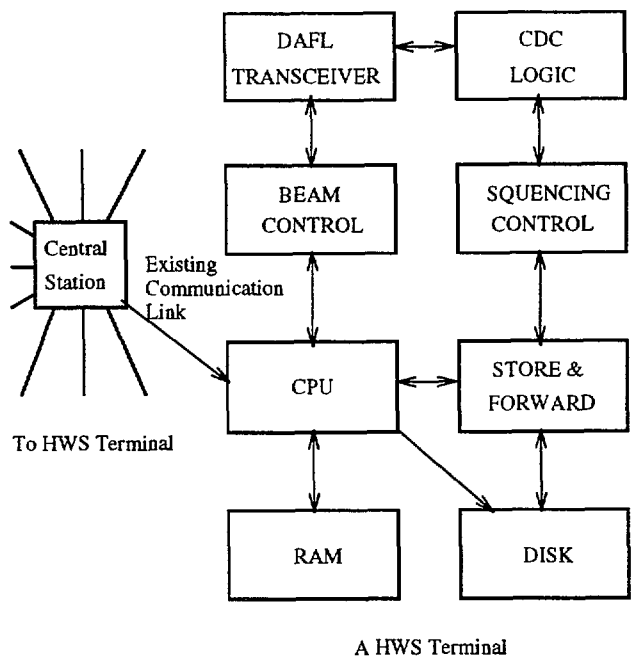

Fig. 7 Intelligent highway communication system design

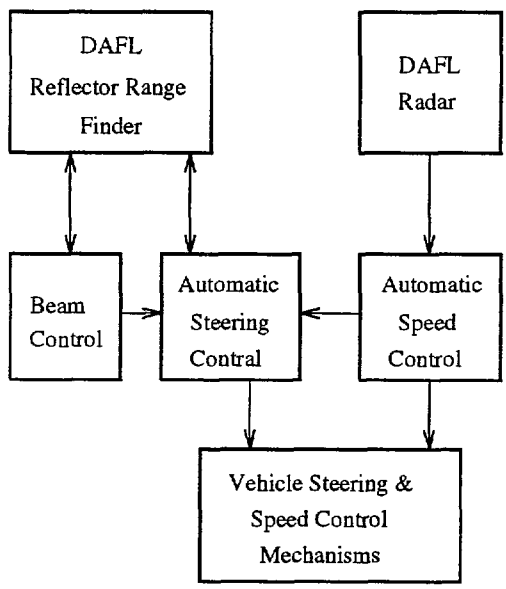

Fig. 8 Vehicle terminal design for automatic driving

Fig. 9 Electronic laser beam control radiation patterns

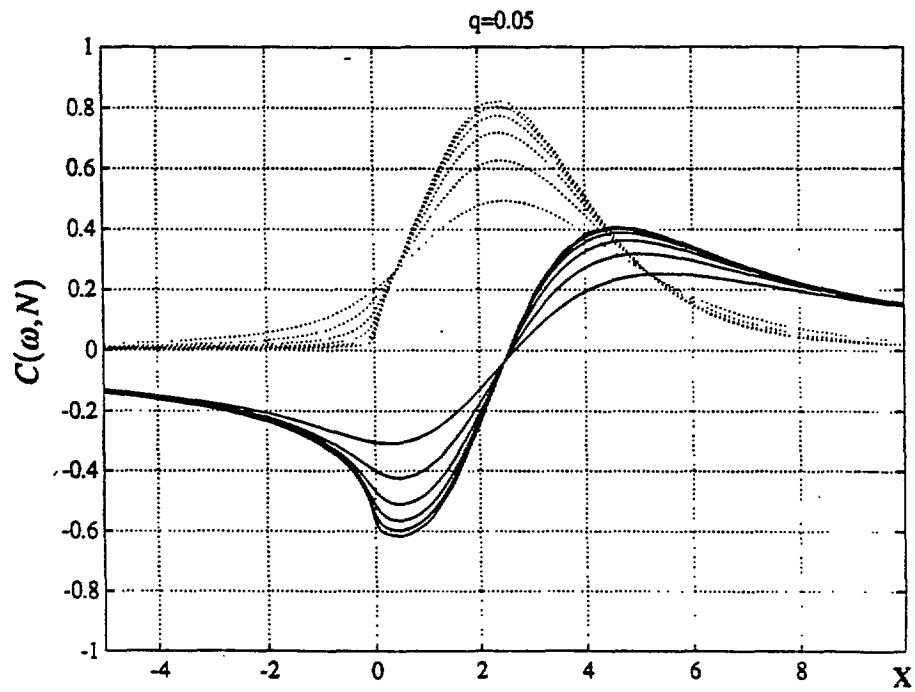

FIGURE *10* Carrier density coefficients of the index of refraction versus the lightwave frequency variable x.— real component (phase) .....imaginary component (gain). The various curves represent parametric dependence on the temperature - relaxation time parameter.

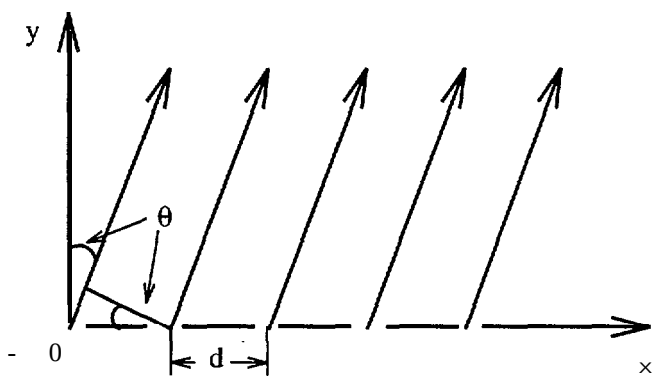

Fig. f l PCC channel output openings.
Arrows indicate direction of radiation

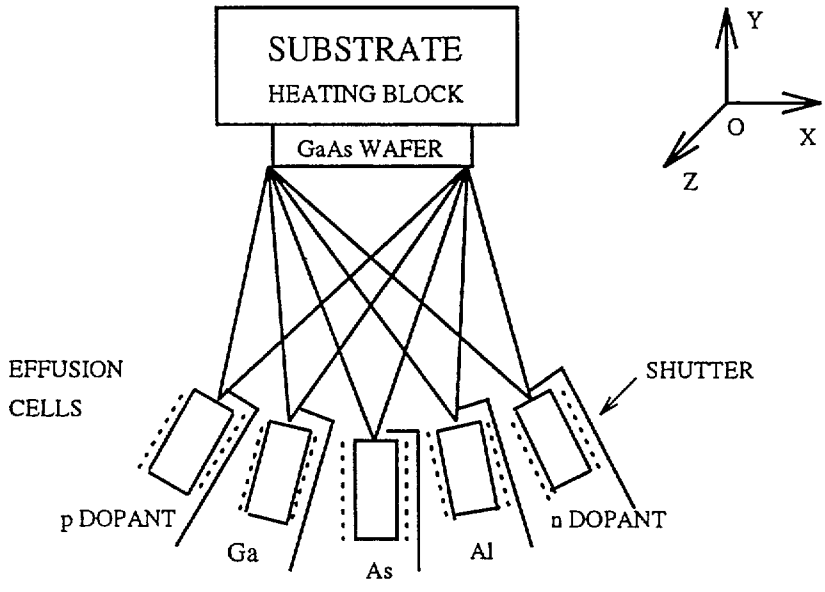

Fig. 12 Schematic diagram of the MBE process for the growth of p- and n-type AlxGa1-xAs